arXiv:hep-ph/0606025v4 9 Aug 2006

PQCD Calculation for $\Lambda_b \to \Lambda\gamma$ in the Standard Model

Xiao-Gang He[1,2], Tong Li[1], Xue-Qian Li[1], and Yu-Ming Wang[1]

[1]Department of Physics, Nankai University, Tianjin

[2]Center for Theoretical Sciences, Department of Physics, National Taiwan University, Taipei

Abstract:

We calculate the branching ratio of $\Lambda_b \to \Lambda\gamma$ in the standard model using the PQCD method. The predicted branching ratio $B(\Lambda_b \to \Lambda\gamma)$ is about $(4.3 \sim 8.6) \times 10^{-8}$, with reasonable parameter ranges in the heavy baryon distribution amplitude. This branching ratio is much smaller than those obtained in other hadronic model calculations. Future experimental data can provide important information on applicability of the PQCD method to heavy baryon radiative decay.

PACS numbers: 13.30.Ce, 12.38.Bx, 14.20.Mr

I. INTRODUCTION

Rare radiative processes involving $b \to s\gamma$ at quark level are important for understanding the flavor changing structure in the standard model (SM). Exclusive radiative B decays also provide important information about the hadronic matrix elements where a heavy b-quark is involved. These processes being rare can also provide clues to models beyond the SM. There have been considerable studies on inclusive $b \to s\gamma$[1, 2], and exclusive mesonic $B \to K^*\gamma$[3] both experimentally and theoretically within and beyond the SM [4, 5, 6]. Theoretical predictions for inclusive decays agree with data very well in the SM. Calculations for exclusive processes are in general consistent with data although there are unavoidable uncertainties due to our lack of good understanding of QCD at low energies. Nevertheless methods have been developed to calculate hadronic matrix elements in recent years [7, 8]. With more data becoming available, new b-decay processes can be studied. These processes can be new tests for different methods in calculating hadronic matrix elements and new physics beyond the SM. In this work we study $\Lambda_b \to \Lambda\gamma$. In this decay more experimental information about the heavy b quark inside the hadron which is not available in inclusive and mesonic b-hadron decays, such as spin polarization during hadronization, and the handedness of the couplings at the quark level, can be extracted[9, 10, 11, 12, 13]. Therefore the baryonic b-hadron radiative decay can provide a new test for theoretical methods for b-quark hadronization.

There are some studies in the literature on $\Lambda_b \to \Lambda\gamma$[9, 10, 11, 12, 13] decay ranging from phenomenological models to QCD sum rule approaches. Our study will be based on the PQCD method[14, 15, 16]. This method has been shown to give consistent results for two body mesonic B decays[8]. We expect a PQCD calculation for $\Lambda_b \to \Lambda\gamma$ will also give a reasonable estimate since the energy-exchange carried by gluons in the matrix element calculations is large. Result obtained in this way can serve as a good reference for discussing the relevant hadronic matrix elements.

For SM, the effective Hamiltonian responsible for $b \to s\gamma$ comes from the electromagnetic penguin diagram and is given by[17]:

$$H_{eff} \;=\; i\frac{G_F}{2\sqrt{2}}V_{tb}V^*_{ts}\frac{e}{4\pi^2}C_7^{eff}(\mu)m_b\bar{s}\sigma_{\mu\nu}(1+\gamma_5)bF^{\mu\nu}, \tag{1}$$

where $C_7^{eff}(\mu = m_b) = -0.31$. In our numerical calculations, the running of C_7^{eff} will also be taken into account.

It has been shown that there may be resonant (long distance) $J/\psi(\psi')$ contributions[18]. If these contributions are included, one should add a term $(3C_1(\mu) + C_2(\mu))(3/\alpha^2_{em})\sum_{j=\psi,\psi'}\omega_j(0)k_j\pi\Gamma(j \to l^+l^-)M_j/(q^2 - M_j^2 + iM_j\Gamma_j^{tot})$ to the Wilson coefficient C_7^{eff}. Since for $b \to s\gamma$ process, $q^2 = 0$, there are double suppressions for the long distance resonant contributions with one of them coming from the Breit-Wigner factor $\sim \Gamma_i/M_i$ and another coming from the extrapolation of $\omega_j(M_i^2) = 1$ to $\omega_j(0)$ with $\omega_j(0) < 0.13$ (and could be smaller)[18], we will neglect the resonant contribution for radiative decays in our later discussions.

At the hadron level, the decay amplitude for $\Lambda_b \to \Lambda\gamma$ is obtained by inserting the effective Hamiltonian between the initial and final hadron states,

$$M(\Lambda_b \to \Lambda\gamma) = \langle\Lambda\gamma|H_{eff}|\Lambda_b\rangle. \tag{2}$$

There are two form factors for $\Lambda_b \to \Lambda\gamma$ from the above which we write as

$$M_\mu \;\equiv \langle\Lambda(p')|C_7^{eff}(\mu,0)\bar{s}\sigma_{\mu\nu}q^\nu(1+\gamma_5)b|\Lambda_b(p)\rangle = \overline{\Lambda(p')}(F_L\sigma_{\mu\nu}q^\nu(1-\gamma_5) + F_R\sigma_{\mu\nu}q^\nu(1+\gamma_5))\Lambda_b(p). \tag{3}$$

We obtain

$$\Gamma(\Lambda_b \to \Lambda\gamma) = \frac{G_F^2|V_{tb}|^2|V_{ts}|^2\alpha_{em}|C_7^{eff}|^2m_b^2}{32m^3_{\Lambda_b}\pi^4}(m^2_{\Lambda_b} - m^2_\Lambda)^3(|F_L|^2 + |F_R|^2). \tag{4}$$

Emission of a photon from the tree operators $O_{1,2}$ can also contribute to $\Lambda_b \to \Lambda\gamma$. Although the Wilson coefficients of these operators are larger than those of the penguin operators, there is a large suppression coming from the CKM factor $|V_{ub}V^*_{us}/V_{tb}V^*_{ts}|$. The overall contributions from bremsstrahlung of a photon off the operator $O_{1,2}$ is therefore suppressed. We will neglect their contribution in rest of discussions.

II. PQCD CALCULATION OF THE HADRONIC MATRIX ELEMENTS

We now describe our calculations for the hadronic matrix elements defined above using the PQCD method developed in Ref.[14, 15, 16]. We define, in the rest frame of Λ_b, p, p' to be the Λ_b, Λ momenta, $k_i (i = 1, 2, 3)$ to be the valence quark momenta inside Λ_b, and k'_i to be the valence quark momenta inside Λ. We parameterize the light cone momenta with all light quark and baryon masses neglected as

$$
\begin{aligned}
&p = (p^+, p^-, \mathbf{0}_T) = \frac{M_{\Lambda_b}}{\sqrt{2}}(1, 1, \mathbf{0}_T), \;\; p' = (p'^+, 0, \mathbf{0}_T) \\
&k_1 = (p^+, x_1 p^-, \mathbf{k}_{1T}), \;\; k_2 = (0, x_2 p^-, \mathbf{k}_{2T}), \;\; k_3 = (0, x_3 p^-, \mathbf{k}_{3T}) \\
&k'_1 = (x'_1 p'^+, 0, \mathbf{k}'_{1T}), \;\; k'_2 = (x'_2 p'^+, 0, \mathbf{k}'_{2T}), \;\; k'_3 = (x'_3 p'^+, 0, \mathbf{k}'_{3T})
\end{aligned}
\tag{5}
$$

where x_i and x'_i are the fractions of the longitudinal momenta of the valence quarks with $x_1 + x_2 + x_3 = 1$ and $x'_1 + x'_2 + x'_3 = 1$. $\mathbf{k}_{iT}$ and $\mathbf{k}'_{iT}$ are the transverse momenta of the valence quarks inside Λ_b and Λ, respectively.

As a self-consistent check, one should make sure that the expected relation $p^2 - k_1^2 \sim 0(\Lambda_{QCDm_b})$ holds, since the light quarks in the heavy baryon should have momenta of order Λ_{QCD}. Naively, the above gives a value of order $(1 - x_2)m^2_{\Lambda_b}$ which does not have the explicit form as expected. To understand this, one needs to combine the form of the heavy baryon wavefunction which determines how quark momenta are distributed inside the baryon. We have checked this using the wavefunction given later, and obtained the ratio of average values $< x_{2,3} > / < x_1 >\sim m/m_{\Lambda_b}$, where m is of order Λ_{QCD}. With the constraint $x_1 + x_2 + x_3 = 1$, the desired order for $p^2 - k_1^2$ is then obtained.

One can write $p'^+ = \rho p^+$ with $\rho = \frac{2p\cdot p'}{M^2_{\Lambda_b}} = \frac{p^2+p'^2-q^2}{M^2_{\Lambda_b}}$. The ranges for q^2 and ρ are given by $0 \le q^2 \le (M_{\Lambda_b} - m_\Lambda)^2$ and $2m_\Lambda/M_{\Lambda_b} \le \rho \le (M^2_{\Lambda_b} + m^2_\Lambda)/M^2_{\Lambda_b}$ if off-shell photon is allowed. In our case of $\Lambda_b \to \Lambda\gamma$, $q^2 = 0$. Here we have kept Λ mass in the expressions for the purpose in tracing the ranges of the kinematic variables. In the approximation we are using, it should be set to zero as mentioned above.

In the PQCD picture, hadrons are formed from quarks with appropriate wave functions describing the momenta distribution of quarks inside the hadron. The Λ_b wave function is usually defined through the quantity [19, 20].

$$
\begin{aligned}
(Y_{\Lambda_b})_{\alpha\beta\gamma}(k_i, \nu) &= \frac{1}{2\sqrt{2}N_c}\int\prod_{l=2}^{3}\frac{dw_l^+ d\mathbf{w_l}}{(2\pi)^3}e^{ik_l w_l}\varepsilon^{abc}\langle 0|T[b^a_\alpha(0)u^b_\beta(w_2)d^c_\gamma(w_3)]|\Lambda_b(p)\rangle \\
&= \frac{f_{\Lambda_b}}{8\sqrt{2}N_c}[(\not{p} + M_{\Lambda_b})\gamma_5 C]_{\beta\gamma}[\Lambda_b(p)]_\alpha \Psi(k_i, \nu),
\end{aligned}
\tag{6}
$$

where f_{Λ_b} is a normalization constant, $\Lambda_b(p)$ is the Λ_b spinor, and $\Psi(k_i, \mu)$ is the wave function. Here we have used the heavy quark symmetry which should be applicable in the present case, following Refs.[19, 20], to reduce the form factors to the above simplified form. In general there are more components in the wavefunction if all quarks are light. For the light baryon Λ the leading-twist wave function of Λ is defined by[24]:

$$
\begin{aligned}
(Y_\Lambda)_{\alpha\beta\gamma}(k'_i, \nu) &= \frac{1}{2\sqrt{2}N_c}\int\prod_{l=1}^{2}\frac{dw_l^- d\mathbf{w_l}}{(2\pi)^3}e^{ik'_l w_l}\varepsilon^{abc}\langle 0|T[s^a_\alpha(w_1)u^b_\beta(w_2)d^c_\gamma(0)]|\Lambda(p')\rangle \\
&= \frac{f_\Lambda}{8\sqrt{2}N_c}\{(\not{p}'C)_{\beta\gamma}[\gamma_5\Lambda(p')]_\alpha\Phi^V(k'_i, \nu) + (\not{p}'\gamma_5 C)_{\beta\gamma}[\Lambda(p')]_\alpha\Phi^A(k'_i, \nu)\} \\
&- \frac{f^T_\Lambda}{8\sqrt{2}N_c}(\sigma_{\mu\nu}p'^\nu C)_{\beta\gamma}[\gamma^\mu\gamma_5\Lambda(p')]_\alpha\Phi^T(k'_i, \nu),
\end{aligned}
\tag{7}
$$

where f_Λ and f^T_Λ are normalization constants, and $\Lambda(p')$ is the Λ spinor.

Including the Sudakov factor with infrared cut-offs $\omega(\omega')$, and running the wavefunction from ν down to $\omega(\omega')$, then we obtain[14]:

$$
\begin{aligned}
\Psi(x_i, b_i, p, \nu) &= \exp[-\sum_{l=2}^{3}s(\omega, x_l p^-) - 3\int_\omega^\nu\frac{d\overline{\mu}}{\overline{\mu}}\gamma_q(\alpha_s(\overline{\mu}))]\Psi(x_i) \\
\Phi^j(x'_i, b'_i, p', \nu) &= \exp[-\sum_{l=1}^{3}s(\omega', x'_l p^+) - 3\int_{\omega'}^\nu\frac{d\overline{\mu}}{\overline{\mu}}\gamma_q(\alpha_s(\overline{\mu}))]\Phi^j(x'_i),
\end{aligned}
\tag{8}
$$

where $j = V,\ A,\ T$, $\omega = min(1/\tilde{b}_1, 1/\tilde{b}_2, 1/\tilde{b}_3)$, and $\omega' = min(1/\tilde{b}'_1, 1/\tilde{b}'_2, 1/\tilde{b}'_3)$. $\tilde{b}_1^{(')} = |\mathbf{b}_2^{(')} - \mathbf{b}_3^{(')}|$, $\tilde{b}_2^{(')} = |\mathbf{b}_1^{(')} - \mathbf{b}_3^{(')}|$, and $\tilde{b}_3^{(')} = |\mathbf{b}_1^{(')} - \mathbf{b}_2^{(')}|$. Here $\mathbf{b}$ and $\mathbf{b}'$ are the conjugate variables to $\mathbf{k}_T$ and $\mathbf{k}'_T$ defined in Appendix B.

The explicit expressions for the Sudakov factors are given in Ref.[14] with

$$\begin{aligned}
&s(\omega, Q) = \int_{\omega}^{Q} \frac{dp}{p}[ln(\frac{Q}{p})A[\alpha_s(p)] + B[\alpha_s(p)]] \\
&A = C_F \frac{\alpha_s}{\pi} + [\frac{67}{9} - \frac{\pi^2}{3} - \frac{10}{27}n_f + \frac{8}{3}\beta_0 ln(\frac{e^{\gamma_E}}{2})](\frac{\alpha_s}{\pi})^2 \\
&B = \frac{2}{3}\frac{\alpha_s}{\pi} ln(\frac{e^{2\gamma_E - 1}}{2}) \\
&\gamma_q(\alpha_s(\mu)) = -\alpha_s(\mu)/\pi, \\
&\beta_0 = \frac{33 - 2n_f}{12},
\end{aligned} \tag{9}$$

where γ_E is the Euler constant. n_f is the flavor number, and γ_q is the anomalous dimension. For Λ_b baryon decays, the typical energy scale is above the charm mass. We will take n_f equal to 4 in our calculations.

The hadronic matrix elements can be written as:

$$\begin{aligned}
&M_{l,\mu} = \int [Dx] \int [Db] (\overline{Y}_{\Lambda})_{\alpha'\beta'\gamma'}(x_i', b_i', p', \nu) \\
&H_{l,\mu}^{\alpha'\beta'\gamma'\alpha\beta\gamma}(x_i, x_i', b_i, b_i', M_{\Lambda_b}, \nu)(Y_{\Lambda_b})_{\alpha\beta\gamma}(x_i, b_i, p, \nu),
\end{aligned} \tag{10}$$

where the measures of the momentum fractions [14] are give by

$$[Dx] = [dx][dx'], \;\; [dx] = dx_1 dx_2 dx_3 \delta(1 - \sum_{l=1}^{3} x_l), \;\; [dx'] = dx_1' dx_2' dx_3' \delta(1 - \sum_{l=1}^{3} x_l'). \tag{11}$$

The measures of the transverse extents $[Db]$ are defined in Appendix A.

The hard scattering amplitude $H_{l,\mu}^{\alpha'\beta'\gamma'\alpha\beta\gamma}(x, x', b, b', M_{\Lambda_b}, \nu)$ is obtained by first evaluating the amplitude $H_{l,\mu}^{i,\alpha'\beta'\gamma'\alpha\beta\gamma}(x_i, x_i', \mathbf{k}_T, \mathbf{k}_T', M_{\Lambda_b})$ for the 'i'th diagram in Fig. 1 for a corresponding Wilson coefficient C_l^{eff} which is displayed in Appendix B. One then carries out a Fourier transformation on $\mathbf{k}_T$ and $\mathbf{k}_T'$ to $\vec{b}$ and $\vec{b}'$ space to obtain $\tilde{H}_{l,\mu}^{i,\alpha'\beta'\gamma'\alpha\beta\gamma}(x, x', b, b', M_{\Lambda_b})$. The procedure of carrying out this transformation is described at the end of Appendix B.

Collecting all contributions in Fig.1 and multiplying the corresponding Wilson coefficients, one then obtains a hard scattering amplitude $H_{l,\mu}^{\alpha'\beta'\gamma'\alpha\beta\gamma}(x, x', b, b', M_{\Lambda_b}) = \sum_i C_l^{eff}(t)\tilde{H}_{l,\mu}^{i,\alpha'\beta'\gamma'\alpha\beta\gamma}(x, x', b, b', M_{\Lambda_b})$. Here we have labelled the hard scale as t which is taken to be the larger of the two variables $t_{1,2}$ associated with the virtual gluon momentum in Fig. 1, i.e. $t = \max(t_1^i, t_2^i)$. The expressions for $t_{1,2}$ are listed in Appendix C.

Finally a RG running is applied to the hard scattering amplitude to match the scale ν in the wave functions and we obtain[14]

$$\begin{aligned}
&H_{l,\mu}^{\alpha'\beta'\gamma'\alpha\beta\gamma}(x, x', b, b', M_{\Lambda_b}, \nu) = \\
&\exp[-6\int_{\nu}^{t} \frac{d\overline{\mu}}{\overline{\mu}}\gamma_q(\alpha_s(\overline{\mu}))] \times H_{l,\mu}^{\alpha'\beta'\gamma'\alpha\beta\gamma}(x, x', b, b', M_{\Lambda_b})
\end{aligned} \tag{12}$$

The form factors are obtained by grouping relevant terms according to the definition in eq. (3). Using eq.(10) we obtain a generic expression for the form factors corresponding to each diagram as

$$\begin{aligned}
F_l^i \;&=\; \sum_{j=V,A,T} \frac{\pi^2}{27} f_{\Lambda}^j f_{\Lambda_b} \int [Dx] \int [Db]^i C_l^{eff}(t^i) \\
&\quad \Psi_{\Lambda_b}(x)\Phi_{\Lambda}^j(x')\exp[-S^i] H_F^{ij}\Omega^i \\
S \;&=\; \sum_{k=2}^{3} s(\omega, x_k p^-) + \sum_{k=1}^{3} s(\omega', x_k' p'^+) + 3\int_{\omega}^{t}\frac{d\overline{\mu}}{\overline{\mu}}\gamma_q(\alpha_s(\overline{\mu})) + 3\int_{\omega'}^{t}\frac{d\overline{\mu}}{\overline{\mu}}\gamma_q(\alpha_s(\overline{\mu}))
\end{aligned} \tag{13}$$

where F_l^i represents the form factors contributed by the "i" the diagram in which operators with the Wilson coefficients C_l^{eff} are inserted, in our case $C_l^{eff} = C_7^{eff}$. The superscript j labels V, A, and T related to the spin structure of the valence quarks in the Λ baryon with $f_{\Lambda}^A = f_{\Lambda}^V = f_{\Lambda}$. The explicit expressions of Ω^i are presented in Appendix D. The functions H_F^{ij} are given in Appendix E. The total form factors are obtained by summing over contributions from all diagrams.

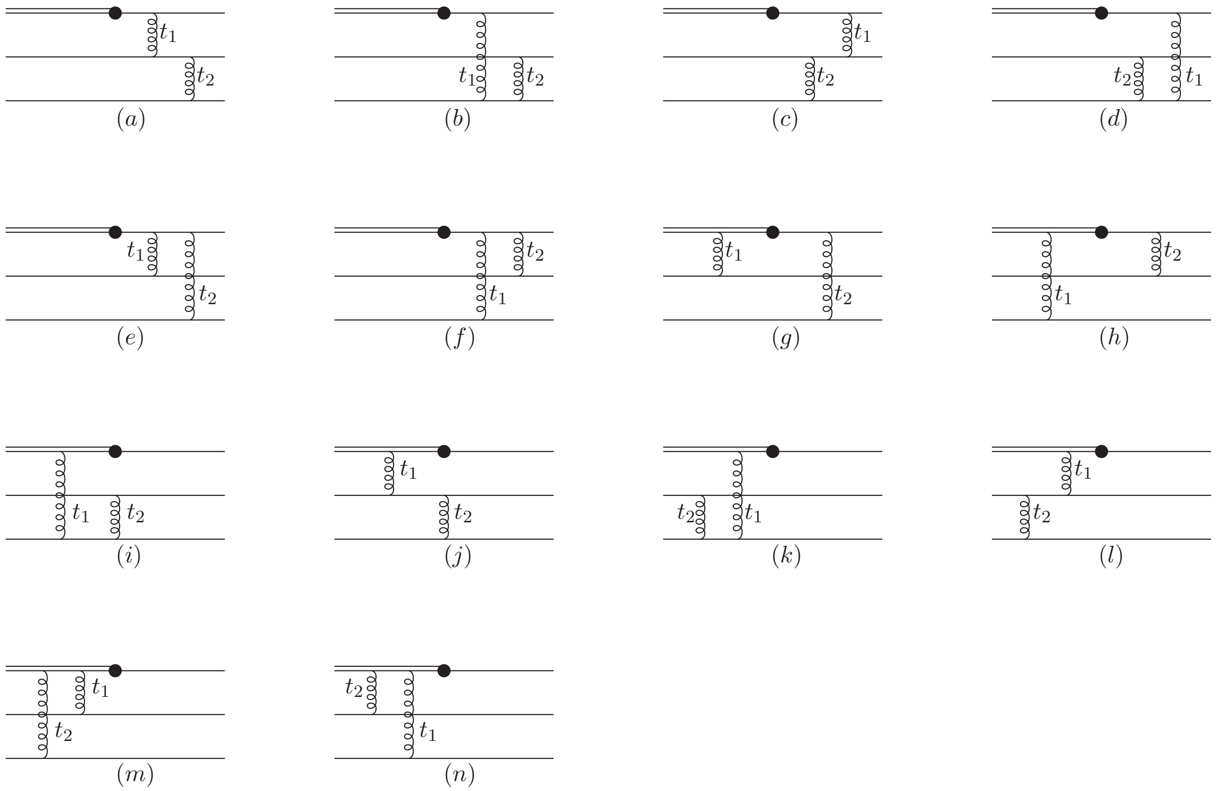

FIG. 1: The lowest order diagrams for the $\Lambda_b \to \Lambda\gamma$ decay. The solid lines, double lines, wavy lines and the black blub vertex denote the light quarks, b quark, gluon and the electromagnetic penguin vertex, respectively. Diagrams with triple-gluon vertex do not contribute since their color factors are all zero in the present case.

III. NUMERICAL RESULTS

We are now ready to evaluate the form factors numerically. For concreteness, we adopt the model proposed in Ref.[19] for the Λ_b baryon distribution amplitude Ψ,

$$\Psi(x_1, x_2, x_3) = N x_1 x_2 x_3 \exp[-\frac{M_{\Lambda_b}^2}{2\beta^2 x_1} - \frac{m_q^2}{2\beta^2 x_2} - \frac{m_q^2}{2\beta^2 x_3}]. \tag{14}$$

The normalization constant N is obtained by the condition:

$$\int [dx]\Psi(x_1, x_2, x_3) = 1. \tag{15}$$

The decay constant f_{Λ_b} is determined by fitting $B(\Lambda_b \to \Lambda_c l\overline{\nu})$ whose central value is 5% measured by DELPHI[21] using the same PQCD method. When fitting the data we truncate the double log Sudakov factor in such a way that the factor exp(-s) is smaller than 1 following the prescription in Ref.[22]. Our numbers for f_{Λ_b} are different from those obtained in Ref.[15] where a $B(\Lambda_b \to \Lambda_c l\overline{\nu})$ was taken to be 2%. We also have chosen cut-offs as $\omega = 1.14 min(1/\tilde{b}_1, 1/\tilde{b}_2, 1/\tilde{b}_3)$ and $\omega' = 1.14 min(1/\tilde{b}'_1, 1/\tilde{b}'_2, 1/\tilde{b}'_3)$. The factor 1.14 is adopted because this cut-off choice can result in form factors which vary smoothly with square of momentum transfer in fitting $\Lambda_b \to \Lambda_c l\overline{\nu}$ process and it reflects the resummation of next-to-leading double log in higher order radiative corrections[23]. Also the β and m_q in the heavy baryon wavefunction distribution need to be fixed. In Ref.[14, 15, 16], $\beta = 1$ GeV and $m_q = 0.3$ GeV were used to estimate $\Lambda_b \to \Lambda_c l\bar{\nu}$, $\Lambda_b \to p l\bar{\nu}$ and also $\Lambda_b \to \Lambda J/\psi$ decay rates. β should not be too much smaller than 1 GeV if the form factors are dominated by perturbative contributions. Therefore we will let both β and m_q vary within ranges as $0.6 \sim 1$GeV and $0.2 \sim 0.3$GeV. The results for f_{Λ_b} are shown in Table I for different parameter choices respectively.

The Λ baryon distribution amplitudes have been studied using QCD sum rules. In this work, we adopt the model

TABLE I: Decay constant f_{Λ_b} for different choices of β and m_q, respectively.

f_{Λ_b}(GeV)	$\beta = 0.6$GeV	$\beta = 0.7$GeV	$\beta = 0.8$GeV	$\beta = 0.9$GeV	$\beta = 1$GeV
$m_q = 0.2$GeV	0.691×10^{-3}	0.841×10^{-3}	1.02×10^{-3}	1.21×10^{-3}	1.43×10^{-3}
$m_q = 0.3$GeV	1.27×10^{-3}	1.45×10^{-3}	1.65×10^{-3}	1.88×10^{-3}	2.12×10^{-3}

proposed in Ref.[24],

$$\begin{aligned}
&\phi^V(x_1,x_2,x_3) = 42\phi_{as}(x_1,x_2,x_3)[0.18(x_3^2 - x_2^2) + 0.10(x_2 - x_3)],\\
&\phi^A(x_1,x_2,x_3) = -42\phi_{as}(x_1,x_2,x_3)[0.26(x_3^2 + x_2^2) + 0.34x_1^2 - 0.56x_2x_3 - 0.24x_1(x_2 + x_3)],\\
&\phi^T(x_1,x_2,x_3) = 42\phi_{as}(x_1,x_2,x_3)[1.2(x_2^2 - x_3^2) - 1.4(x_2 - x_3)],\\
&\phi_{as}(x_1,x_2,x_3) = 120x_1x_2x_3. \qquad (16)
\end{aligned}$$

The asymmetric distribution in the momentum fractions of the three quarks implies $SU(3)$ symmetry breaking.

The constants f_Λ and f_Λ^T are fixed to be[24]

$$f_\Lambda = 0.63 \times 10^{-2}\text{GeV}^2, \;\; f_\Lambda^T = 0.063 \times 10^{-2}\text{GeV}^2. \qquad (17)$$

Finally to obtain the branching ratio for $\Lambda_b \to \Lambda\gamma$, for definitiveness we fix rest of the parameters as following. The parameter Λ_{QCD} which enters in the strong coupling constant and various Wilson coefficients, the b quark mass and the CKM mixing parameters are set to be: Λ_{QCD} at 0.2 GeV, $m_b = 4.8$ GeV, and the CKM mixing parameters are set to their central values[25]: $s_{12} = 0.2243$, $s_{23} = 0.00413$, $s_{13} = 0.0037$ and $\delta_{13} = 1.05$.

Our explicit calculations show that $F_L = 0$ and a non-zero value for F_R as expected since light quark and light baryon masses have been neglected. The contributions from each diagrams for F_R are shown in Appendix E. The resulting branching ratio is shown in Table II. We see that the branching ratio for $\Lambda_b \to \Lambda\gamma$ is in the range of $(4.3 \sim 6.8) \times 10^{-8}$.

TABLE II: Branching ratio(BR) of $\Lambda_b \to \Lambda\gamma$ for different choices of β and m_q with Sudakov truncation.

BR($\times 10^8$)	$\beta = 0.6$GeV	$\beta = 0.7$GeV	$\beta = 0.8$GeV	$\beta = 0.9$GeV	$\beta = 1$GeV
$m_q = 0.2$GeV	6.76	6.26	6.19	4.90	4.67
$m_q = 0.3$GeV	6.42	5.75	5.61	4.44	4.32

IV. DISCUSSIONS AND CONCLUSIONS

In this work we have used the perturbative QCD approach to evaluate the branching ratio for radiative decay $\Lambda_b \to \Lambda\gamma$. This process occurs via penguin diagrams. Our results are shown in Table II. The branching ratio obtained is much smaller than results obtained, shown in Table III, using other methods.

TABLE III: Decay branching ratios (B) of $\Lambda_b \to \Lambda\gamma$ based on the form factors from the QCD sum rule approach, the covariant oscillator quark model, HQET and MIT bag model, respectively

Model	pole model[10]	QCD sum rule[11]	covariant oscillator quark model[12]	HQET[13]	bag model[13]
B	$(0.10 \sim 0.45) \times 10^{-5}$	$(3.7 \pm 0.5) \times 10^{-5}$	0.23×10^{-5}	$(1.2 \sim 1.9) \times 10^{-5}$	0.6×10^{-5}

There are uncertainties in PQCD predictions due to unknown parameters in wavefunctions. We have tried to understand such uncertainties by varying several relevant parameters. Within reasonable ranges of the parameters it is not possible to obtain a branching ratio larger than 10^{-7}. We have considered another possible uncertainty in the method used here. This is the choice of the infrared cut-offs $\omega(\omega')$ in the Sudakov suppression factor which damps the perturbative contributions. In our calculations the cut-offs are set to the conventional values with $\omega = 1.14min(1/\tilde{b}_1, 1/\tilde{b}_2, 1/\tilde{b}_3)$ and $\omega' = 1.14min(1/\tilde{b}'_1, 1/\tilde{b}'_2, 1/\tilde{b}'_3)$ discussed in the text. The factor 1.14 is adopted because this choice for cut-offs' can result in form factors which vary smoothly with square of momentum transfer in fitting $\Lambda_b \to \Lambda_c l \overline{\nu}$ process and it reflects the resummation of next-to-leading double log in higher order radiative corrections[23]. We have checked with slightly different cut-offs and find impossible to obtain branching ratio to be as large as what listed in Table III.

The prescription of truncating the factor exp(-s) to be smaller than 1 described in Ref.[22] may also be a source for uncertainties. We therefore have evaluated the branching ratio without this truncation. The results are shown in Table IV. We see that the results are similar to those obtained in Table II.

TABLE IV: Branching ratio(BR) of $\Lambda_b \to \Lambda\gamma$ for different choices of β and m_q without Sudakov truncation.

BR($\times 10^8$)	$\beta = 0.6$GeV	$\beta = 0.7$GeV	$\beta = 0.8$GeV	$\beta = 0.9$GeV	$\beta = 1$GeV
$m_q = 0.2$GeV	8.60	7.22	5.91	4.92	4.60
$m_q = 0.3$GeV	5.96	5.73	5.70	4.67	4.30

We therefore conclude that within the PQCD framework, the branching ratio for $\Lambda_b \to \Lambda\gamma$ is much smaller than other model calculations. This is somewhat surprising since PQCD calculation for the branching ratio of $B \to K^{(*)}\gamma$ obtains a value of order consistent to other model calculations and also agrees with experimental value of about 4×10^{-5}[6]. There is a huge suppression for $\Lambda_b \to \Lambda\gamma$. At this moment there is no data available for $\Lambda_b \to \Lambda\gamma$ yet. One has to wait for future experimental data to tell us more. If a branching ratio above 10^{-7} is measured at some future facilities, such as LHCb, the PQCD method used here will certainly need to be modified.

On the theoretical side, one expects the branching ratio for $\Lambda_b \to \Lambda\gamma$ to be smaller than that of $B \to K^{(*)}\gamma$ due to several suppression factors such as an additional α_s^2 and a large momentum squared q^2 suppression factor as one more hard gluon is exchanged between quarks. There is also an additional Sudakov suppression factor due to an additional spectator quark involved in the process as can be seen from eq.(13).

One might question the applicability of PQCD method for the process under consideration. One notes that in the PQCD approach, both gluons are hard ones which excludes the possibility of including contributions where two spectator quarks (not involved in the weak interaction vertex) form a collective object first due to soft gloun exchanges, i.e. the diquark, and then this object interacts with the other quark by exchanging a hard gluon. If this contribution turns out to be the dominant one, the branching ratio may be substantially larger. At present there is no solid theoretical method to treat this effect yet, we do not have a definitive answer about this. We, however, note that estimate for $\Lambda_b \to \Lambda J/\psi$ using the same method gives a reasonable range compared with data[16]. This can be taken as a support for the applicability of the method to Λ_b decays. Our result for $B(\Lambda_b \to \Lambda\gamma)$ represents a reasonable estimate. The branching ratio for $\Lambda_b \to \Lambda\gamma$ is in the range of $(4.3 \sim 8.6) \times 10^{-8}$ which is smaller than predictions using other methods listed in Table III. We have to wait for future experiments to provide more information.

Acknowledgements:

This work is supported in part by NNSFC, NSC and NCTS. We would like to thank Hsiang-nan Li and Cai-Dian Lü for helpful discussions. We also thank H.n. Li for providing us with the program for numerical integration.

Appendix A: the b measures

The ordinary b measure is defined as

$$[d\mathbf{b}] = \frac{d^2\mathbf{b}}{(2\pi)^2} \tag{18}$$

The explicit forms of $[D\mathbf{b}]^i$ for each diagram i in Fig. 1 are given by

$$\begin{aligned}
&[D\mathbf{b}]^{(a)} = [d\mathbf{b}_1][d\mathbf{b}_3][d\mathbf{b}'_1][d\mathbf{b}'_3], && [D\mathbf{b}]^{(b)} = [d\mathbf{b}_1][d\mathbf{b}_2][d\mathbf{b}'_1][d\mathbf{b}'_2],\\
&[D\mathbf{b}]^{(c)} = [d\mathbf{b}_1][d\mathbf{b}_3][d\mathbf{b}'_1][d\mathbf{b}'_3], && [D\mathbf{b}]^{(d)} = [d\mathbf{b}_1][d\mathbf{b}_2][d\mathbf{b}'_1][d\mathbf{b}'_2],\\
&[D\mathbf{b}]^{(e)} = [d\mathbf{b}_2][d\mathbf{b}'_2][d\mathbf{b}'_3], && [D\mathbf{b}]^{(f)} = [d\mathbf{b}_3][d\mathbf{b}'_2][d\mathbf{b}'_3],\\
&[D\mathbf{b}]^{(g)} = [d\mathbf{b}_2][d\mathbf{b}_3][d\mathbf{b}'_3], && [D\mathbf{b}]^{(h)} = [d\mathbf{b}_2][d\mathbf{b}_3][d\mathbf{b}'_2]\\
&[D\mathbf{b}]^{(i)} = [d\mathbf{b}_1][d\mathbf{b}_2][d\mathbf{b}'_1][d\mathbf{b}'_2], && [D\mathbf{b}]^{(j)} = [d\mathbf{b}_1][d\mathbf{b}_3][d\mathbf{b}'_1][d\mathbf{b}'_3],\\
&[D\mathbf{b}]^{(k)} = [d\mathbf{b}_1][d\mathbf{b}_2][d\mathbf{b}'_1][d\mathbf{b}'_2], && [D\mathbf{b}]^{(l)} = [d\mathbf{b}_1][d\mathbf{b}_3][d\mathbf{b}'_1][d\mathbf{b}'_3],\\
&[D\mathbf{b}]^{(m)} = [d\mathbf{b}_2][d\mathbf{b}_3][d\mathbf{b}'_2], && [D\mathbf{b}]^{(n)} = [d\mathbf{b}_2][d\mathbf{b}_3][d\mathbf{b}'_3].
\end{aligned} \tag{19}$$

Appendix B: Hard scattering amplitudes $H^{i,\alpha'\beta'\gamma'\alpha\beta\gamma}_{l,\mu}(x_i, x'_i, \mathbf{k}_T, \mathbf{k}'_T, M_{\Lambda_b})$

Expressions of amplitude $H^{i,\alpha'\beta'\gamma'\alpha\beta\gamma}_{l,\mu}(x_i, x'_i, \mathbf{k}_T, \mathbf{k}'_T, M_{\Lambda_b})$ for each diagram in Fig. 1. In the following O^l_μ comes from the γ-matrix in the effective Hamiltonian, $O^{l=7}_\mu = \sigma_{\mu\nu} q^\nu R$

For the hard amplitude of Fig.1(a):

$$\begin{aligned}
&H^{a,\alpha'\beta'\gamma'\alpha\beta\gamma}_{\mu}(x_i, x'_i, \mathbf{k}_T, \mathbf{k}'_T, M_{\Lambda_b}) = \\
&[\varepsilon^{abc}\varepsilon^{a'b'c'}(T^j)_{c'c}(T^jT^i)_{b'b}(T^i)_{a'a}]g_s^4 \frac{(\gamma_\rho)_{\gamma'\gamma}[\gamma^\rho(\not{p}' - \not{k}'_1 - \not{k}_3)\gamma^\lambda]_{\beta'\beta}[\gamma_\lambda(\not{p}' - \not{p} + \not{k}_1)O_\mu]_{\alpha'\alpha}}{(p' - k'_1 - k_3)^2(p' - p + k_1)^2(p - p' + k'_1 - k_1)^2(k_3 - k'_3)^2} \\
&= C_N g_s^4 \frac{(\gamma_\rho)_{\gamma'\gamma}[\gamma^\rho(\not{p}' - \not{k}'_1 - \not{k}_3)\gamma^\lambda]_{\beta'\beta}[\gamma_\lambda(\not{p}' - \not{p} + \not{k}_1)O_\mu]_{\alpha'\alpha}}{[A_a + (\mathbf{k}'_{1T} + \mathbf{k}_{3T})^2][B_a + \mathbf{k}^2_{1T}][C_a + (\mathbf{k}_{1T} - \mathbf{k}'_{1T})^2][D_a + (\mathbf{k}_{3T} - \mathbf{k}'_{3T})^2]}
\end{aligned} \tag{20}$$

with

$$A_a = x_3(1 - x'_1)\rho M^2_{\Lambda_b}, B_a = (1 - x_1)\rho M^2_{\Lambda_b}, C_a = (1 - x_1)(1 - x'_1)\rho M^2_{\Lambda_b}, D_a = x_3 x'_3 \rho M^2_{\Lambda_b} \tag{21}$$

and the color factor

$$C_N = \varepsilon^{abc}\varepsilon^{a'b'c'}(T^j)_{c'c}(T^jT^i)_{b'b}(T^i)_{a'a} = \frac{(N^2 - 1)(N + 1)}{12} \tag{22}$$

For the hard amplitude of Fig.1(b):

$$\begin{aligned}
&H^{b,\alpha'\beta'\gamma'\alpha\beta\gamma}_{\mu}(x_i, x'_i, \mathbf{k}_T, \mathbf{k}'_T, M_{\Lambda_b}) = \\
&[\varepsilon^{abc}\varepsilon^{a'b'c'}(T^iT^j)_{c'c}(T^i)_{b'b}(T^j)_{a'a}]g_s^4 \frac{(\gamma^\rho)_{\beta'\beta}[\gamma_\rho(\not{p}' - \not{k}'_1 - \not{k}_2)\gamma_\lambda]_{\gamma'\gamma}[\gamma^\lambda(\not{p}' - \not{p} + \not{k}_1)O_\mu]_{\alpha'\alpha}}{(p' - k'_1 - k_2)^2(p' - p + k_1)^2(p - p' - k_1 + k'_1)^2(k'_2 - k_2)^2} \\
&= C_N g_s^4 \frac{(\gamma^\rho)_{\beta'\beta}[\gamma_\rho(\not{p}' - \not{k}'_1 - \not{k}_2)\gamma_\lambda]_{\gamma'\gamma}[\gamma^\lambda(\not{p}' - \not{p} + \not{k}_1)O_\mu]_{\alpha'\alpha}}{[A_b + (\mathbf{k}'_{1T} + \mathbf{k}_{2T})^2][B_b + \mathbf{k}^2_{1T}][C_b + (\mathbf{k}_{1T} - \mathbf{k}'_{1T})^2][D_b + (\mathbf{k}_{2T} - \mathbf{k}'_{2T})^2]}
\end{aligned} \tag{23}$$

with

$$A_b = x_2(1 - x'_1)\rho M^2_{\Lambda_b}, B_b = (1 - x_1)\rho M^2_{\Lambda_b}, C_b = (1 - x_1)(1 - x'_1)\rho M^2_{\Lambda_b}, D_b = x_2 x'_2 \rho M^2_{\Lambda_b} \tag{24}$$

Inspection of the above calculations, one notices that one can easily obtain $H^{b,\alpha'\beta'\gamma'\alpha\beta\gamma}_{\mu}(x_i, x'_i, \mathbf{k}_T, \mathbf{k}'_T, M_{\Lambda_b})$ from $H^{a,\alpha'\beta'\gamma'\alpha\beta\gamma}_{\mu}(x_i, x'_i, \mathbf{k}_T, \mathbf{k}'_T, M_{\Lambda_b})$ and vice versa by simply exchanging the momentum indices 2 and 3 for $\mathbf{k}$ and $\mathbf{k}'$, and exchanging the positions of the Dirac indices $\gamma'\gamma$ and $\beta'\beta$. Due to these properties, the contributions to the form factors from the above two diagrams are the same. This fact can be easily understood by noticing the following properties of the quantities related to the distribution amplitudes: i) The distribution amplitudes $\Psi(x_1, x_2, x_3)$, and $\phi^A(x_1, x_2, x_3)$ are symmetric in exchanging x_2 and x_3, while $\phi^{V,T}(x_1, x_2, x_3)$ are anti-symmetric in exchanging x_2 and x_3, as can be seen from eqs.(14) and (16). And ii) When exchanging the Dirac indices β and γ, the expressions for $(Y_{\Lambda_b})_{\alpha\beta\gamma}(k_i\nu)$ in eq.(6), and terms proportional to ϕ^A for $(Y_\Lambda)_{\alpha\beta\gamma}(k'_i, \nu)$ in eq.(7) will have a sign change, while terms proportional to $\phi^{V,T}$ remain the same. Since going from the contribution of diagram (a) to diagram (b) involves both actions: exchanging the momentum indices 2 and 3, and the Dirac indices β and γ, this results in no sign changes for all the terms involved. After integrating out $x(x')_{2,3}$ and $b(b')_{2,3}$ to obtain the final form factors using eq.(13), one then obtains the same results for both diagrams (a) and (b).

Similar situation happens for the following pairs of diagrams: (c) and (d), (e) and (f), (g) and (h), (i) and (j), (k) and (l), and, (m) and (n). In the following we will only display the results for diagrams (a), (c), (e), (g), (i), (k) and (m). The expressions for diagrams (b), (d), (f), (h), (j), (l) and (n) can be obtained by exchanging $x(x')_2$ and $x(x')_3$, and also $\gamma'\gamma$ and $\beta'\beta$.

For the hard amplitude of Fig.1(c):

$$\begin{aligned}
&H^{c,\alpha'\beta'\gamma'\alpha\beta\gamma}_{\mu}(x_i, x'_i, \mathbf{k}_T, \mathbf{k}'_T, M_{\Lambda_b}) = \\
&[\varepsilon^{abc}\varepsilon^{a'b'c'}(T^j)_{c'c}(T^iT^j)_{b'b}(T^i)_{a'a}]g_s^4 \frac{(\gamma_\rho)_{\gamma'\gamma}[\gamma^\lambda(\not{p} - \not{k}_1 - \not{k}'_3)\gamma^\rho]_{\beta'\beta}[\gamma_\lambda(\not{p}' - \not{p} + \not{k}_1)O_\mu]_{\alpha'\alpha}}{(p - k_1 - k'_3)^2(p' - p + k_1)^2(p - p' + k'_1 - k_1)^2(k_3 - k'_3)^2} \\
&= C_N g_s^4 \frac{(\gamma_\rho)_{\gamma'\gamma}[\gamma^\lambda(\not{p} - \not{k}_1 - \not{k}'_3)\gamma^\rho]_{\beta'\beta}[\gamma_\lambda(\not{p}' - \not{p} + \not{k}_1)O_\mu]_{\alpha'\alpha}}{[A_c + (\mathbf{k}_{1T} + \mathbf{k}'_{3T})^2][B_c + \mathbf{k}^2_{1T}][C_c + (\mathbf{k}_{3T} - \mathbf{k}'_{3T})^2][D_c + (\mathbf{k}_{1T} - \mathbf{k}'_{1T})^2]}
\end{aligned} \tag{25}$$

with

$$A_c = x'_3(1 - x_1)\rho M^2_{\Lambda_b}, B_c = (1 - x_1)\rho M^2_{\Lambda_b}, C_c = x_3 x'_3 \rho M^2_{\Lambda_b}, D_c = (1 - x_1)(1 - x'_1)\rho M^2_{\Lambda_b} \tag{26}$$

For the hard amplitude of Fig.1(e):

$$\begin{aligned}
&H_\mu^{e,\alpha'\beta'\gamma'\alpha\beta\gamma}(x_i,x_i',\mathbf{k}_T,\mathbf{k}_T',M_{\Lambda_b})=\\
&[\varepsilon^{abc}\varepsilon^{a'b'c'}(T^i)_{c'c}(T^iT^j)_{b'b}(T^j)_{a'a}]g_s^4\frac{(\gamma_\rho)_{\gamma'\gamma}[\gamma^\rho(\not{p}'-\not{k}_2'-\not{k}_3)\gamma^\lambda(\not{p}'-\not{p}+\not{k}_1)O_\mu]_{\alpha'\alpha}(\gamma_\lambda)_{\beta'\beta}}{(p'-k_2'-k_3)^2(p'-p+k_1)^2(k_2'-k_2)^2(k_3-k_3')^2}\\
&=C_N g_s^4\frac{(\gamma_\rho)_{\gamma'\gamma}[\gamma^\rho(\not{p}'-\not{k}_2'-\not{k}_3)\gamma^\lambda(\not{p}'-\not{p}+\not{k}_1)O_\mu]_{\alpha'\alpha}(\gamma_\lambda)_{\beta'\beta}}{[A_e+(\mathbf{k}_{2T}'+\mathbf{k}_{3T})^2][B_e+\mathbf{k}_{1T}^2][C_e+(\mathbf{k}_{2T}-\mathbf{k}_{2T}')^2][D_e+(\mathbf{k}_{3T}-\mathbf{k}_{3T}')^2]}
\end{aligned}\tag{27}$$

with

$$A_e=x_3(1-x_1')\rho M_{\Lambda_b}^2, B_e=(1-x_1)\rho M_{\Lambda_b}^2, C_e=x_2x_2'\rho M_{\Lambda_b}^2, D_e=x_3x_3'\rho M_{\Lambda_b}^2\tag{28}$$

For the hard amplitude of Fig.1(g):

$$\begin{aligned}
&H_\mu^{g,\alpha'\beta'\gamma'\alpha\beta\gamma}(x_i,x_i',\mathbf{k}_T,\mathbf{k}_T',M_{\Lambda_b})=\\
&[\varepsilon^{abc}\varepsilon^{a'b'c'}(T^i)_{c'c}(T^j)_{b'b}(T^iT^j)_{a'a}]g_s^4\frac{(\gamma_\rho)_{\gamma'\gamma}[\gamma^\rho(\not{p}'-\not{k}_2'-\not{k}_3)O_\mu(\not{p}-\not{k}_3-\not{k}_2'+m_b)\gamma^\lambda]_{\alpha'\alpha}(\gamma_\lambda)_{\beta'\beta}}{[(p-k_3-k_2')^2-m_b^2](p'-k_2'-k_3)^2(k_2'-k_2)^2(k_3'-k_3)^2}\\
&=C_N g_s^4\frac{(\gamma_\rho)_{\gamma'\gamma}[\gamma^\rho(\not{p}'-\not{k}_2'-\not{k}_3)O_\mu(\not{p}-\not{k}_3-\not{k}_2'+m_b)\gamma^\lambda]_{\alpha'\alpha}(\gamma_\lambda)_{\beta'\beta}}{[A_g+(\mathbf{k}_{2T}'+\mathbf{k}_{3T})^2][B_g+(\mathbf{k}_{2T}'+\mathbf{k}_{3T})^2][C_g+(\mathbf{k}_{2T}-\mathbf{k}_{2T}')^2][D_g+(\mathbf{k}_{3T}-\mathbf{k}_{3T}')^2]}
\end{aligned}\tag{29}$$

with

$$A_g=(x_2'(1-x_3)\rho+x_3)M_{\Lambda_b}^2, B_g=x_3(1-x_2')\rho M_{\Lambda_b}^2, C_g=x_2x_2'\rho M_{\Lambda_b}^2, D_g=x_3x_3'\rho M_{\Lambda_b}^2\tag{30}$$

For the hard amplitude of Fig.1(i):

$$\begin{aligned}
&H_\mu^{i,\alpha'\beta'\gamma'\alpha\beta\gamma}(x_i,x_i',\mathbf{k}_T,\mathbf{k}_T',M_{\Lambda_b})=\\
&[\varepsilon^{abc}\varepsilon^{a'b'c'}(T^iT^j)_{c'c}(T^i)_{b'b}(T^j)_{a'a}]g_s^4\frac{[\gamma_\rho(\not{p}'-\not{k}_1'-\not{k}_2)\gamma_\lambda]_{\gamma'\gamma}[O_\mu(\not{p}-\not{p}'-\not{k}_1'+m_b)\gamma^\lambda]_{\alpha'\alpha}(\gamma^\rho)_{\beta'\beta}}{[(p-p'+k_1')^2-m_b^2](p'-k_1'-k_2)^2(p-p'-k_1+k_1')^2(k_2'-k_2)^2}\\
&=C_N g_s^4\frac{[\gamma_\rho(\not{p}'-\not{k}_1'-\not{k}_2)\gamma_\lambda]_{\gamma'\gamma}[O_\mu(\not{p}-\not{p}'-\not{k}_1'+m_b)\gamma^\lambda]_{\alpha'\alpha}(\gamma^\rho)_{\beta'\beta}}{[A_i+(\mathbf{k}_{2T}+\mathbf{k}_{1T}')^2][B_i+(\mathbf{k}_{1T}'+\mathbf{k}_{2T})^2][C_i+(\mathbf{k}_{1T}-\mathbf{k}_{1T}')^2][D_i+(\mathbf{k}_{2T}-\mathbf{k}_{2T}')^2]}
\end{aligned}\tag{31}$$

with

$$A_i=(1-x_1')\rho M_{\Lambda_b}^2, B_i=x_2(1-x_1')\rho M_{\Lambda_b}^2, C_i=(1-x_1)(1-x_1')\rho M_{\Lambda_b}^2, D_i=x_2x_2'\rho M_{\Lambda_b}^2\tag{32}$$

For the hard amplitude of Fig.1(k):

$$\begin{aligned}
&H_\mu^{k,\alpha'\beta'\gamma'\alpha\beta\gamma}(x_i,x_i',\mathbf{k}_T,\mathbf{k}_T',M_{\Lambda_b})=\\
&[\varepsilon^{abc}\varepsilon^{a'b'c'}(T^iT^j)_{c'c}(T^j)_{b'b}(T^i)_{a'a}]g_s^4\frac{[\gamma_\rho(\not{p}-\not{k}_1-\not{k}_2')\gamma_\lambda]_{\gamma'\gamma}[O_\mu(\not{p}-\not{p}'+\not{k}_1'+m_b)\gamma^\rho]_{\alpha'\alpha}(\gamma^\lambda)_{\beta'\beta}}{[(p-p'+k_1')^2-m_b^2](p-k_1-k_2')^2(p-p'-k_1+k_1')^2(k_2'-k_2)^2}\\
&=C_N g_s^4\frac{[\gamma_\rho(\not{p}-\not{k}_1-\not{k}_2')\gamma_\lambda]_{\gamma'\gamma}[O_\mu(\not{p}-\not{p}'+\not{k}_1'+m_b)\gamma^\rho]_{\alpha'\alpha}(\gamma^\lambda)_{\beta'\beta}}{[A_k+\mathbf{k}_{1T}'^2][B_k+(\mathbf{k}_{1T}+\mathbf{k}_{2T}')^2][C_k+(\mathbf{k}_{1T}-\mathbf{k}_{1T}')^2][D_k+(\mathbf{k}_{2T}-\mathbf{k}_{2T}')^2]}
\end{aligned}\tag{33}$$

with

$$A_k=(1-x_1')\rho M_{\Lambda_b}^2, B_k=x_2'(1-x_1)\rho M_{\Lambda_b}^2, C_k=(1-x_1)(1-x_1')\rho M_{\Lambda_b}^2, D_k=x_2x_2'\rho M_{\Lambda_b}^2\tag{34}$$

For the hard amplitude of Fig.1(m):

$$\begin{aligned}
&H_\mu^{m,\alpha'\beta'\gamma'\alpha\beta\gamma}(x_i,x_i',\mathbf{k}_T,\mathbf{k}_T',M_{\Lambda_b})=\\
&[\varepsilon^{abc}\varepsilon^{a'b'c'}(T^j)_{c'c}(T^i)_{b'b}(T^iT^j)_{a'a}]g_s^4\frac{(\gamma_\lambda)_{\gamma'\gamma}[O_\mu(\not{p}-\not{p}'+\not{k}_1'+m_b)\gamma_\rho(\not{p}-\not{k}_2-\not{k}_3'+m_b)\gamma^\lambda]_{\alpha'\alpha}(\gamma^\rho)_{\beta'\beta}}{[(p-p'+k_1')^2-m_b^2][(p-k_2-k_3')^2-m_b^2](k_2'-k_2)^2(k_3'-k_3)^2}\\
&=C_N g_s^4\frac{(\gamma_\lambda)_{\gamma'\gamma}[O_\mu(\not{p}-\not{p}'+\not{k}_1'+m_b)\gamma_\rho(\not{p}-\not{k}_2-\not{k}_3'+m_b)\gamma^\lambda]_{\alpha'\alpha}(\gamma^\rho)_{\beta'\beta}}{[A_m+\mathbf{k}_{1T}'^2][B_m+(\mathbf{k}_{2T}+\mathbf{k}_{3T}')^2][C_m+(\mathbf{k}_{2T}-\mathbf{k}_{2T}')^2][D_m+(\mathbf{k}_{3T}-\mathbf{k}_{3T}')^2]}
\end{aligned}\tag{35}$$

with

$$A_m = (1-x_1')\rho M_{\Lambda_b}^2, B_m = (x_3'(1-x_2)\rho + x_2)M_{\Lambda_b}^2, C_m = x_2 x_2' \rho M_{\Lambda_b}^2, D_m = x_3 x_3' \rho M_{\Lambda_b}^2 \tag{36}$$

The expressions for the hard scattering amplitude in b and b' space are obtained by making a Fourier transformation on k_T and k_T' space. In the following we given one example for Fig.1(a) as an illustration. We note that the k_T and k_T' dependencies are all in the denominators in the above expressions, one then just needs to consider that part of the fourier transformation. For Fig.1(a), it is given by

$$\Omega^{(a)}(x_i, x_i', \mathbf{k}_T, \mathbf{k}_T', M_{\Lambda_b}) = \frac{1}{[A_a + (\mathbf{k}_{1T}' + \mathbf{k}_{3T})^2][B_a + \mathbf{k}_{1T}^2][C_a + (\mathbf{k}_{1T} - \mathbf{k}_{1T}')^2][D_a + (\mathbf{k}_{3T} - \mathbf{k}_{3T}')^2]}. \tag{37}$$

The fourier transformed expression is then given by

$$\Omega^{(a)}(x_i, x_i', b_i, b_i', M_{\Lambda_b}) = \int e^{-i(\mathbf{k}_{1T}\cdot\mathbf{b}_1 + \mathbf{k}_{1T}'\cdot\mathbf{b}_1' + \mathbf{k}_{3T}\cdot\mathbf{b}_3 + \mathbf{k}_{3T}'\cdot\mathbf{b}_3')}\Omega^{(a)}(x_i, x_i', \mathbf{k}_T, \mathbf{k}_T', M_{\Lambda_b}) d^2\mathbf{k}_{1T} d^2\mathbf{k}_{1T}' d^2\mathbf{k}_{3T} d^2\mathbf{k}_{3T}'. \tag{38}$$

Defining $\mathbf{k}_{AT} \equiv \mathbf{k}_{1T}' + \mathbf{k}_{3T}$, $\mathbf{k}_{BT} \equiv \mathbf{k}_{1T}$, $\mathbf{k}_{CT} \equiv \mathbf{k}_{1T} - \mathbf{k}_{1T}'$, and $\mathbf{k}_{DT} \equiv \mathbf{k}_{3T} - \mathbf{k}_{3T}'$, we rewrite the transformation as

$$\begin{aligned}
&\Omega^{(a)}(x_i, x_i', b_i, b_i', M_{\Lambda_b}) \\
&= \int \frac{e^{-i[\mathbf{k}_{AT}\cdot(\mathbf{b}_3+\mathbf{b}_3') + \mathbf{k}_{BT}\cdot(\mathbf{b}_1+\mathbf{b}_1'-\mathbf{b}_3-\mathbf{b}_3') + \mathbf{k}_{CT}\cdot(-\mathbf{b}_1'+\mathbf{b}_3+\mathbf{b}_3') + \mathbf{k}_{DT}\cdot(-\mathbf{b}_3')]}1}{(\mathbf{k}_{AT}^2 + A_a)(\mathbf{k}_{BT}^2 + B_a)(\mathbf{k}_{CT}^2 + C_a)(\mathbf{k}_{DT}^2 + D_a)} d^2\mathbf{k}_{AT} d^2\mathbf{k}_{BT} d^2\mathbf{k}_{CT} d^2\mathbf{k}_{DT} \\
&= (2\pi)^4 K_0(\sqrt{A_a}|b_3 + b_3'|) K_0(\sqrt{B_a}|b_1 + b_1' - b_3 - b_3'|) K_0(\sqrt{C_a}|b_1' - b_3 - b_3'|) K_0(\sqrt{D_a}|b_3'|),
\end{aligned} \tag{39}$$

In the above we have used

$$\int d^2k \frac{e^{i\mathbf{k}\cdot\mathbf{b}}}{k^2 + A} = 2\pi K_0(\sqrt{A}|\mathbf{b}|), A > 0. \tag{40}$$

One obtains the expression for $H_\mu^{a,\alpha'\beta'\gamma'\alpha\beta\gamma}(x_i, x_i', b, b', M_{\Lambda_b})$ as

$$H_\mu^{a,\alpha'\beta'\gamma'\alpha\beta\gamma}(x_i, x_i', b, b', M_{\Lambda_b}) = C_N g_s^4 (\gamma_\rho)_{\gamma'\gamma} [\gamma^\rho (\not{p}' - \not{k}_1' - \not{k}_3)\gamma^\lambda]_{\beta'\beta} [\gamma_\lambda (\not{p}' - \not{p} + \not{k}_1) O_\mu]_{\alpha'\alpha} \widetilde{\Omega^{(a)}}(x_i, x_i', b_i, b_i', M_{\Lambda_b}). \tag{41}$$

In carrying out the fourier transformations for other diagrams, two other forms of functions will be encountered. We list them in the following

$$\begin{aligned}
&\int d^2k \frac{e^{i\mathbf{k}\cdot\mathbf{b}}}{(k^2 + A)(k^2 + B)} = \pi \int_0^1 dz \frac{|\mathbf{b}| K_1(\sqrt{Z_1}|\mathbf{b}|)}{\sqrt{Z_1}}, A, B > 0, \\
&\int d^2k_1 d^2k_2 \frac{e^{i(\mathbf{k}_1\cdot\mathbf{b}_1 + \mathbf{k}_2\cdot\mathbf{b}_2)}}{(k_1^2 + A)(k_2^2 + B)[(k_1 + k_2)^2 + C]} = \pi^2 \int_0^1 \frac{dz_1 dz_2}{z_1(1-z_1)} \frac{\sqrt{X_2}}{\sqrt{|Z_2|}} K_1(\sqrt{X_2 Z_2}),
\end{aligned} \tag{42}$$

where $A > 0$ and B, C arbitrary. K_0 and K_1 are the modified Bessel functions of the second kind. And

$$\begin{aligned}
Z_1 &= Az + B(1-z), \\
Z_2 &= A(1-z_2) + \frac{z_2}{z_1(1-z_1)}[B(1-z_1) + Cz_1], \\
X_2 &= (\mathbf{b}_1 - z_1\mathbf{b}_2)^2 + \frac{z_1(1-z_1)}{z_2}\mathbf{b}_2^2
\end{aligned} \tag{43}$$

Appendix C: The maximum of $t_{1,2}$

The hard scales, the maximal of t_1^i and t_2^i for diagrams (a), (c), (e), (g), (i), (k), and (m) in Fig. 1. Exchanging $b(b')_2$ and $b(b')_3$, one obtains the expressions for diagrams (b), (d), (f), (h), (j), (l) and (n). The expressions of C_i, D_i are collected in Appendix B.

Appendix D: Expressions of Ω^i

The expression of Ω^i for diagrams (a), (c), (e), (g), (i), (k), and (m) in Fig. 1. Exchanging $b(b')_2$ and $b(b')_3$, one

i	t_1^i	t_2^i
(a)	$\max\{\sqrt{\vert C_a\vert}, \frac{1}{\vert\mathbf{b}_1'-\mathbf{b}_3-\mathbf{b}_3'\vert}, \omega, \omega'\}$	$\max\{\sqrt{\vert D_a\vert}, \frac{1}{\vert\mathbf{b}_3'\vert}, \omega, \omega'\}$
(c)	$\max\{\sqrt{\vert C_c\vert}, \frac{1}{\vert\mathbf{b}_1'\vert}, \omega, \omega'\}$	$\max\{\sqrt{\vert D_c\vert}, \frac{1}{\vert\mathbf{b}_3\vert}, \omega, \omega'\}$
(e)	$\max\{\sqrt{\vert C_e\vert}, \frac{1}{\vert\mathbf{b}_2'\vert}, \omega, \omega'\}$	$\max\{\sqrt{\vert D_e\vert}, \frac{1}{\vert\mathbf{b}_3'\vert}, \omega, \omega'\}$
(g)	$\max\{\sqrt{\vert C_g\vert}, \frac{1}{\vert\mathbf{b}_2\vert}, \omega, \omega'\}$	$\max\{\sqrt{\vert D_g\vert}, \frac{1}{\vert\mathbf{b}_3'\vert}, \omega, \omega'\}$
(i)	$\max\{\sqrt{\vert C_i\vert}, \frac{1}{\vert\mathbf{b}_1\vert}, \omega, \omega'\}$	$\max\{\sqrt{\vert D_i\vert}, \frac{1}{\vert\mathbf{b}_2'\vert}, \omega, \omega'\}$
(k)	$\max\{\sqrt{\vert C_k\vert}, \frac{1}{\vert\mathbf{b}_1-\mathbf{b}_2-\mathbf{b}_2'\vert}, \omega, \omega'\}$	$\max\{\sqrt{\vert D_k\vert}, \frac{1}{\vert\mathbf{b}_2\vert}, \omega, \omega'\}$
(m)	$\max\{\sqrt{\vert C_m\vert}, \frac{1}{\vert\mathbf{b}_2'\vert}, \omega, \omega'\}$	$\max\{\sqrt{\vert D_m\vert}, \frac{1}{\vert\mathbf{b}_3\vert}, \omega, \omega'\}$

obtains the expressions for diagrams (b), (d), (f), (h), (j), (l) and (n).

$$
\begin{aligned}
\Omega^{(a)} &= (2\pi)^4 K_0(\sqrt{A_a}|\mathbf{b}_3+\mathbf{b}_3'|)K_0(\sqrt{B_a}|\mathbf{b}_1+\mathbf{b}_1'-\mathbf{b}_3-\mathbf{b}_3'|)K_0(\sqrt{C_a}|\mathbf{b}_1'-\mathbf{b}_3-\mathbf{b}_3'|)K_0(\sqrt{D_a}|\mathbf{b}_3'|)\\
\Omega^{(c)} &= (2\pi)^4 K_0(\sqrt{A_c}|\mathbf{b}_3+\mathbf{b}_3'|)K_0(\sqrt{B_c}|\mathbf{b}_1+\mathbf{b}_1'+\mathbf{b}_3+\mathbf{b}_3'|)K_0(\sqrt{C_c}|\mathbf{b}_1'|)K_0(\sqrt{D_c}|\mathbf{b}_3|)\\
\Omega^{(e)} &= 8\pi^5\int_0^1 dz_1dz_2\frac{1}{z_1(1-z_1)}\frac{\sqrt{X_2^e}}{\sqrt{|Z_2^e|}}K_1(\sqrt{X_2^eZ_2^e})K_0(\sqrt{D_e}|\mathbf{b}_3'|)\\
\Omega^{(g)} &= 16\pi^5\int_0^1 dz\frac{|\mathbf{b}_3+\mathbf{b}_3'|K_1(\sqrt{Z_1^g}|\mathbf{b}_3+\mathbf{b}_3'|)}{\sqrt{Z_1^g}}K_0(\sqrt{C_g}|\mathbf{b}_2|)K_0(\sqrt{D_g}|\mathbf{b}_3'|)\\
\Omega^{(i)} &= (2\pi)^4 K_0(\sqrt{A_i}|\mathbf{b}_1+\mathbf{b}_1'-\mathbf{b}_2-\mathbf{b}_2'|)K_0(\sqrt{B_i}|\mathbf{b}_2+\mathbf{b}_2'|)K_0(\sqrt{C_i}|\mathbf{b}_1|)K_0(\sqrt{D_i}|\mathbf{b}_2'|)\\
\Omega^{(k)} &= (2\pi)^4 K_0(\sqrt{A_k}|\mathbf{b}_1+\mathbf{b}_1'-\mathbf{b}_2-\mathbf{b}_2'|)K_0(\sqrt{B_k}|\mathbf{b}_2+\mathbf{b}_2'|)K_0(\sqrt{C_k}|\mathbf{b}_1-\mathbf{b}_2-\mathbf{b}_2'|)K_0(\sqrt{D_k}|\mathbf{b}_2|)\\
\Omega^{(m)} &= 8\pi^5\int_0^1 dz_1dz_2\frac{1}{z_1(1-z_1)}\frac{\sqrt{X_2^m}}{\sqrt{|Z_2^m|}}K_1(\sqrt{X_2^mZ_2^m})K_0(\sqrt{D_m}|\mathbf{b}_3|)
\end{aligned}
\tag{44}
$$

with

$$
\begin{aligned}
X_2^e &= (\mathbf{b}_2'+z_1\mathbf{b}_2)^2+\frac{z_1(1-z_1)}{z_2}\mathbf{b}_2^2, Z_2^e = A_e(1-z_2)+\frac{z_2}{z_1(1-z_1)}[B_e(1-z_1)+C_ez_1]\\
Z_1^g &= A_gz+B_g(1-z)\\
X_2^m &= (\mathbf{b}_2'+z_1\mathbf{b}_2)^2+\frac{z_1(1-z_1)}{z_2}\mathbf{b}_2^2, Z_2^m = A_m(1-z_2)+\frac{z_2}{z_1(1-z_1)}[B_m(1-z_1)+C_mz_1]
\end{aligned}
\tag{45}
$$

Appendix E: Expressions for H_F^{ij}

In this appendix we list H_F^{ij} corresponding to the form factors defined in eq.(13). We use $\tilde{F}_R^j$ for each diagram. The expressions for diagrams (a), (e), (g), (i), (k), and (m) in Fig. 1, whenever non-zero, are listed in the following. The expressions for diagrams (b), (f), (h), (j), (l) and (n) can be obtained by exchanging $x(x')_2$ and $x(x')_3$ and changing the signs for expressions $F_R^{V,T}$. Diagrams (c) and (d) have no contributions to $\Lambda_b \to \Lambda\gamma$. $\tilde{F}_L$ is equal to zero in our approximation.

For the hard amplitudes of Fig.1(a):

$$
\widetilde{F_R^A} = 8x_3\rho^2M_{\Lambda_b}^4 \tag{46}
$$

The relation between the tilde form factors listed above and the form factors in eq.(3) is as the following, taking $\tilde{F}_R^A$ as an example, $F_R^A = \frac{\pi^2}{27}f_\Lambda^j f_{\Lambda_b}\int[Dx]\int[Db]^iC_l^{eff}(t^i)\Psi_{\Lambda_b}(x)\Phi_\Lambda^j(x')\text{exp}[-S^i]\tilde{F}_R^A\Omega^i$. For this example $j = A$, and $f_\Lambda^A = f_\Lambda$. For Fig.1(a), 'i' takes the value 'a'. Similar for other form factors and diagrams.

The other non-zero contributions are

$$
\begin{aligned}
Fig.1(e): \quad & \widetilde{F_R^V} = \widetilde{F_R^A} = -4M_{\Lambda_b}^4\rho^2 x_3, \\
Fig.1(g): \quad & \widetilde{F_R^V} = 4M_{\Lambda_b}^3(m_b\rho + M_{\Lambda_b}(-2x_3(-1+\rho) + (1+x'_2(-1+\rho))\rho)) \\
& \widetilde{F_R^A} = 4M_{\Lambda_b}^3(-1+\rho)(m_b + M_{\Lambda_b}(-1+x'_2\rho)), \\
Fig.1(i): \quad & \widetilde{F_R^A} = 8M_{\Lambda_b}^3 x_2(m_b(-1+\rho) + M_{\Lambda_b}(1+(-1+x'_1)\rho)), \\
Fig.1(k): \quad & \widetilde{F_R^A} = 8M_{\Lambda_b}^3 \rho x'_2(m_b + M_{\Lambda_b}(-1+\rho)), \\
Fig.1(m): \quad & \widetilde{F_R^V} = -4M_{\Lambda_b}^2(-m_b^2(-2+\rho) + M_{\Lambda_b} m_b(x_2 - x_2\rho + (-1+x'_1+x'_3)\rho) \\
& \quad + M_{\Lambda_b}^2(-2+(2-x'_1+x'_3)\rho - x'_3\rho^2 + x_2(1+(-1+x'_1)\rho))) \\
& \widetilde{F_R^A} = -4M_{\Lambda_b}^2(m_b^2\rho + M_{\Lambda_b} m_b(-2+x_2(1+\rho)+(-1+x'_1+x'_3)\rho) \\
& \quad + M_{\Lambda_b}^2(2-(2+x'_1+x'_3)\rho + x'_3\rho^2 + x_2(-1+(1+x'_1)\rho)))
\end{aligned} \tag{47}
$$

[1] CLEO Collaboration, M.S. Alam et al., Phys. Rev. Lett. **74** (1995) 2885.

[2] Belle Collaboration, P. Koppenburg et al., Phys.Rev.Lett. **93** (2004) 061803, BABAR Collaboration, B. Aubert et al., arXiv:hep-ex/0507001.

[3] Belle Collaboration, M. Nakao et al., Phys. Rev. **D69** (2004) 112001 ; BABAR Collaboration, B. Aubert et al., Phys. Rev. **D70** (2004) 112006.

[4] S. Bertolini, F. Borzumati and A. Masiero, Phys. Rev. Lett. **59**, (1987) 180; Mikolaj Misiak, Nucl.Phys. **B393** (1993) 23; K. Adel, York-Peng Yao, Phys.Rev **D49**(1994) 4945; Christoph Greub, Tobias Hurth, Daniel Wyler Phys.Rev **D54** (1996) 3350; Nicolas Pott, Phys.Rev **D54** (1996) 938; X.-G. He, C.-S. Li and L.-L. Yang, Phys. Rev. **D71** (2005) 054006; Riccardo Barbieri, G.F. Giudice, Phys.Lett. **B309** (1993) 86; J.L. Hewett, Phys. Rev. Lett. **70** (1993) 1045; V. Barger, M.S. Berger and R.J.N. Phillips, Phys. Rev. Lett. **70** (1993) 1368.

[5] N.G. Deshpande, P. Lo, J. Trampetic, G. Eilam and P. Singer, Phys. Rev. Lett. **59** (1987) 183; N.G. Deshpande, Josip Trampetic and Kuriakose Panose, Phys.Lett.**B214** (1988) 467; H.-N. Li and G.-L. Lin, Phys. Rev. **D60**, (1999) 054001; M. Beneke, T. Feldmann and D. Seidel, Nucl. Phys. **B612** (2001) 25; S. W. Bosch and G. Buchalla, Nucl. Phys. **B621** (2002) 459; Ahmed Ali and A.Y. Parkhomenko Eur.Phys.J **C23** (2002) 89.

[6] M. Matsumori and A.I. Sanda, Y.-Y. Keum, Phys. Rev. **D72** (2005) 014013.

[7] M. Beneke, G. Buchalla, M. Neubert and C.T. Sachrajda, Phys. Rev. Lett. **83** (1999) 1914; Nucl. Phys. **B591** (2000) 313; Nucl. Phys. **B606** (2001) 245.

[8] Yong-Yeon Keum and Hsiang-nan Li, Phys. Rev. **D63** (2001) 074006; Chuan-Hung Chen, Yong-Yeon Keum and Hsiang-nan Li, Phys. Rev. **D64** (2001) 112002; Yong-Yeon Keum, Hsiang-nan Li and A.I. Sanda, Phys. Rev. **D63** (2001) 054008; Chuan-Hung Chen, Yong-Yeon Keum and Hsiang-nan Li, Phys. Rev. **D66** (2002) 054013; Cai-Dian Lü, Kazumasa Ukai and Mao-Zhi Yang, Phys. Rev. **D63** (2001) 074009; Cai-Dian Lü and Mao-Zhi Yang, Eur. Phys. J. **C23** (2002) 275.

[9] C.-K. Chua, X.-G. He and W.-S. Hou, Phys. Rev. **D60**, (1999) 014003.

[10] T. Mannel and S. Recksiegel, J. Phys. **G24** (1998) 979.

[11] Chao-Shang Huang and Hua-Gang Yan, Phys. Rev. **D59** (1999) 114022.

[12] R. Mohanta, A.K. Giri, M.P. Khanna, M. Ishida and S. Ishida, Prog. Theor. Phys. **102** (1999) 645.

[13] H.Y. Cheng, C-Y. Cheung, G-L. Lin, Y.C. Lin, T.-M. Yan and H-L. Yu, Phys. Rev. **D51** (1995) 1199.

[14] Hsien-Hung Shih, Shih-Chang Lee and Hsiang-nan Li, Phys. Rev. **D59** (1999) 094014.

[15] Hsien-Hung Shih, Shih-Chang Lee and Hsiang-nan Li, Phys. Rev. **D61** (2000) 114002.

[16] Chung-Hsien Chou, Hsien-Hung Shih, Shih-Chang Lee and Hsiang-nan Li, Phys. Rev. **D65** (2002) 074030.

[17] G. Buchalla, A.J. Buras and M.E. Lautenbacher, Rev. Mod. Phys. **68** (1996) 1125.

[18] N.G. Deshpande, X.-G. He, J. Trampetic, Phys. Lett. **B367** (1996) 362.

[19] W. Loinaz and R. Akhoury, Phys. Rev. **D53** (1996) 1416; F. Schlumpf, Ph.D. Thesis, Zurich University, 1992, arXiv:hep-ph/9211255.

[20] F. Hussain, J.G. Korner, M. Kramer and G. Thompson, Z. Phys. **C51** (1991) 321.

[21] DELPHI Collaboration, J. Abdallah et al., Phys. Lett. **B585** (2004) 63.

[22] Yong-Yeon Keum, T. Kurimoto, Hsiang-nan Li, Cai-Dian Lü and A. I. Sanda, Phys. Rev. **D69** (2004) 094018.

[23] Bijoy Kundu, Hsiang-nan Li, Jim Samuelsson and Pankaj Jain, Eur. Phys. J. **C8** (1999) 637.

[24] V.L. Chernyak, A.A. Ogloblin and I.R. Zhitnitsky, Z. Phys. **C42** (1989) 569.

[25] S. Eidelman, et al., Particle Data Group, Phys. Lett. **B592** (2004) 1.